

Resonant two-photon absorption of extreme-ultraviolet free-electron-laser radiation in helium

Mitsuru Nagasono,^{1,*} Edlira Suljoti,¹ Annette Pietzsch,¹ Franz Hennies,^{1,†} Michael Wellhöfer,¹ Jon-Tobias Hoefl,¹ Michael Martins,¹ Wilfried Wurth,¹ Rolf Treusch,² Josef Feldhaus,² Jochen R. Schneider,² and Alexander Föhlisch^{1,‡}

¹*Institute für Experimentalphysik Universität Hamburg, Luruper Chaussee 149, 22761 Hamburg, Germany*

²*HASYLAB at DESY, Notkestrasse 85, 22607 Hamburg, Germany*

(Received 14 February 2007; published 18 May 2007)

We have investigated the nonlinear response of helium to intense extreme-ultraviolet radiation from the free-electron laser in Hamburg (FLASH). We observe a spectral feature between 24 and 26 eV electron kinetic energy in photoemission which shows a quadratic fluence dependence. The feature is explained as a result of subsequent processes involving a resonant two-photon absorption process into doubly excited levels of even parity ($N=5$ and 6), radiative decay to the doubly excited states in the vicinity of the He^+ ($N=2$) ionization threshold and finally the photoionization of the inner electron by the radiation of the next microbunches. This observation suggests that even-parity states, which have been elusive to be measured with the low pulse energy of synchrotron radiation sources, can be investigated with the intense radiation of FLASH. This also demonstrates a first step to bring nonlinear spectroscopy into the xuv and soft-x-ray regime.

DOI: [10.1103/PhysRevA.75.051406](https://doi.org/10.1103/PhysRevA.75.051406)

PACS number(s): 32.80.Rm, 32.80.-t, 34.50.Fa, 41.60.Cr

Nonlinear optical processes such as multiphoton absorption, wave mixing, and the dynamical Stark effect are important in physics and chemistry, biology, materials science, and even communication technology. In addition, nonlinear optics is at the forefront of fundamental science [1–3]. This field has been closely linked to the rapid advances of high power laser technology which covers the range from the far infrared to the vacuum ultraviolet. A prominent example is the field of femtochemistry, whereby time-resolved pump-probe spectroscopy reactions are monitored as they unfold—a tool ideally suited to understand the hard-to-capture transition state and the energetic landscape of reaction chemistry [4]. The understanding of transition states is of great value, as more efficient and more selective chemical processes simultaneously reduce unwanted pollutants and improve economic viability.

Until now, nonlinear processes at shorter wavelength, namely the extreme-ultraviolet (xuv) and the soft-x-ray spectral region, could barely be studied due to a lack of high brilliance radiation sources in this spectral range [5–8]. Nevertheless, this spectral regime poses the great advantage that the properties of selected, atomic centers and their local chemical environment can be separately determined, since xuv and soft-x-ray radiation interacts with atomically localized inner shell electrons. This is a crucial feature as soon as we want to disentangle processes in complex systems, where only few atoms actively contribute in a matrix of many others, which actually is the case for most of the materials science, chemistry, and biology. With the free-electron lasers (FEL) for the xuv and x-ray spectral regime, we can now

address these issues and embark on the study of nonlinear optical processes with high element specificity in the xuv and soft-x-ray regime or even structural resolution in the x-ray regime.

Helium, having two electrons and one nucleus, is the simplest neutral prototype of a three-body quantum mechanical system, and two electron (doubly) excited states arise due to electron correlation, which is of considerable experimental and theoretical interest. The doubly excited states of helium have been extensively studied, since the pioneering work with synchrotron radiation light by Madden and Codling [9] and the single-photon processes in helium are well understood [10–22]. Recently, a significant enhancement of doubly excited helium states, which are weak in photoionization spectroscopy [13], has been observed using fluorescence yield spectroscopy [14–18] and metastable atom yield spectroscopy [20,21]. However, few studies for nonlinear optical process induced with intense vuv radiation have been done [5–8,23].

Using FLASH, the Free-Electron Laser in Hamburg, which provides extreme-ultraviolet (xuv) and soft-x-ray radiation, finally between 12 and 200 eV, with gigawatt peak power and micropulses of 20–50 fs duration [24], we have investigated with photoelectron spectroscopy the response of helium to radiation of $h\nu=38.5\pm 0.2$ eV photon energy and pulse energies between 0 and $1.8\ \mu\text{J}$. We find the fingerprint of two-photon absorption of xuv radiation in helium. This is a first step to bring nonlinear spectroscopy into the xuv and soft-x-ray regime.

FLASH was operated at a photon energy of $h\nu=38.5\pm 0.2$ eV with 2 Hz macropulse repetition rate. Each macropulse consists of a train of micropulses $1\ \mu\text{s}$ apart. We have used macropulses with only a single micropulse, i.e., 2 Hz repetition rate, and macropulses with 8 micropulses. The radiation was guided through the monochromator-beamline PG2 [25] and a 700-nm-thick Al filter 530 mm upstream from the focal point. Thus the high harmonic radiation of FLASH [26] was suppressed and its contribution compared to the primary radiation at $h\nu=38.5$ eV was below 5×10^{-9} [27]. The Al filter and the beamline optics (all op-

*Corresponding author. Present address: RIKEN/XFEL Project Head Office, Kouto 1–1–1, Sayo, Hyogo 679–5148, Japan. Email address: nagasono@spring8.or.jp

†Present address: MAX-lab, Lund University, Box 118, 221 00 Lund, Sweden

‡Corresponding author. Email address: alexander.foehlisch@desy.de

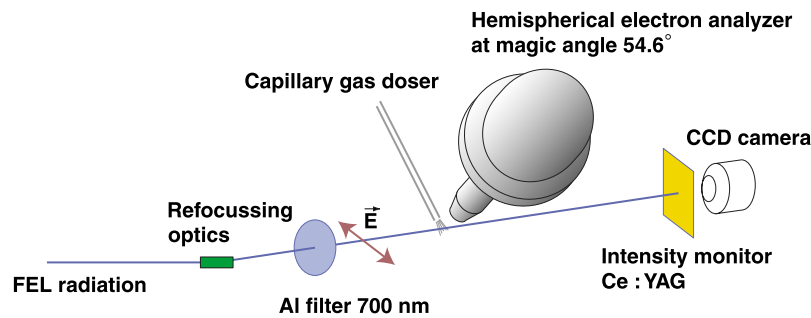


FIG. 1. (Color online) Diagram of the experimental setup. The FEL radiation is focused and spectrally filtered onto the He gas target introduced into the ultrahigh vacuum experimental chamber by a capillary. Photoelectrons are detected by a hemispherical electron analyzer at magic angle detection geometry relative to the linearly polarized radiation with $h\nu=38.5\pm 0.2$ eV photon energy. On a shot-to-shot basis, the photon pulse intensity and the resulting photoelectron spectrum were recorded.

tical elements coated with diamondlike carbon) gave 10% transmission of the primary radiation. Due to the SASE process a shot-to-shot fluctuation of the photon pulse energy between $0 \mu\text{J}$ and up to $1.8 \mu\text{J}$ occurred and was monitored (see below). The experimentally determined focal spot in our ultrahigh vacuum experimental system (base pressure $< 2 \times 10^{-10}$ mbar) was $200 \mu\text{m}^2$.

In Fig. 1 a diagram of the photoemission experiment is shown. Helium was introduced to the experimental chamber at a background pressure of 2×10^{-5} mbar via a copper capillary with an inside diameter of $200 \mu\text{m}$ at 1 mm distance to the focal point. The intensity of the transmitted radiation per macropulse was determined shot-to-shot converting the xuv radiation in a Ce:yttrium aluminum garnet (YAG) crystal into visible light detected by a gated charge-coupled device

(CCD) camera, synchronized to the 2 Hz macropulse repetition rate. The photoelectron spectra were measured at magic angle detection geometry relative to the linearly polarized radiation with a hemispherical electron energy analyzer (Gammadata SES 2002) at a pass energy of 200 eV and an entrance slit size of 2.5 mm. Here, the spectral image was also recorded shot-to-shot by a second gated CCD camera installed in the hemispherical electron analyzer, synchronized to the 2 Hz microbunch repetition rate. Thus, the shot-to-shot images of these two CCD cameras provide photoelectron spectral intensity and photon pulse intensity for each macropulse.

Figure 2(a) shows a He photoelectron spectrum which is accumulated at photon pulse energies ranging from 0.65 to $1.63 \mu\text{J}$, under a condition of helium at 2

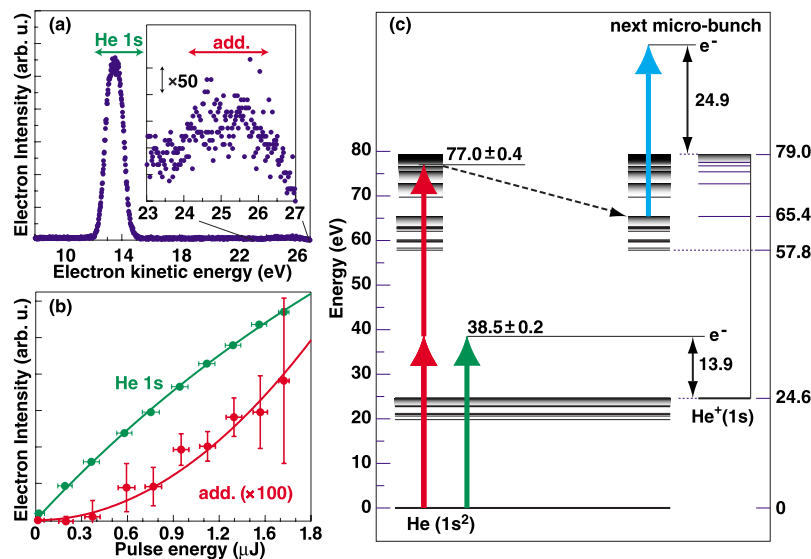


FIG. 2. (Color online) Fluence dependent photoemission of helium with FEL radiation at $h\nu=38.5\pm 0.2$ eV photon energy. (a) Photoelectron spectrum collected at photon pulse energies between $0.65\text{--}1.63 \mu\text{J}/\text{pulse}$ in a $200 \mu\text{m}^2$ focal spot: He 1s photoemission at 13.5 eV kinetic energy, reflecting the He 1s binding energy of 24.6 eV. Inset: additional spectral features between 24–26 eV kinetic energy, not accounted for in single-photon photoemission. (b) Fluence dependence of the He 1s photoemission [upper (green) circles] and spectral features induced by resonant two-photon absorption [lower (red) circles]. Fit of the upper (green) line with a saturation function and of lower (red) line with a quadratic fluence dependence (see text). (c) Energy level diagram of He and He⁺, the single-photon ionization process of the ground state helium [middle (green) arrow], resonant two-photon absorption of the ground state helium [left (red) arrows], direct radiative decay to the vicinity of the He⁺ ($N=2$) ionization threshold (broken arrow), and the single-photon ionization process of doubly excited helium in the vicinity of the He⁺ ($N=2$) ionization threshold (right blue solid arrow).

$\times 10^{-5}$ mbar and in the eight-micropulse mode. The main spectral feature at 13.5 eV electron kinetic energy is the He $1s$ single photon photoionization [Fig. 2(a)]. The photoelectron intensity I_{PE} can be expressed by a saturation function:

$$I_{PE} \propto 1 - \exp\left(\frac{-\sigma I_{hv}}{A}\right), \quad (1)$$

where σ , I_{hv} , and A denote photoionization cross section of helium, pulse energy, and beam size, respectively [28]. The cross section σ is 3.50 Mb/atom at 38 eV [29]. The photoelectron intensity at low pulse energy is proportional to the atomic photoionization cross section and towards high pulse energy saturation due to the depletion of the electronic ground state in the sample volume is observed already at the pulse intensities available in our experiment [Fig. 2(b) upper (green) line]. An additional spectral feature is seen between 24 and 26 eV electron kinetic energy, magnified in the inset to Fig. 2(a). The fluence dependence of this feature is significantly different from the fluence dependence of the one-photon process of He $1s$ photoionization, as shown in Fig. 2(b). The fluence dependence I'_{PE} of this spectral feature can be fitted with a quadratic function [Fig. 2(b), lower (red) line]:

$$I'_{PE} \propto I_{hv}^2. \quad (2)$$

This is the fingerprint of a two-photon process.

At the given photon energy $h\nu=38.5\pm 0.2$ eV the occurrence and the fluence dependence of the additional spectral feature can only be explained as a result of the decay of He double excitation levels of even parity ($N=5$ and 6 ; N is the principal quantum number of the inner electron) converging at 77.0 ± 0.4 eV [13] populated in a resonant two-photon absorption process [Fig. 2(c), left (red) solid arrows]. The two-photon excitation is the first observation in the xuv and soft-x-ray spectral regime, although two-photon ionization of helium has been observed with high harmonic radiation sources based on optical lasers [7,8]. It is important to note that in general even-parity states are forbidden in one-photon absorption in dipole approximation, although in some specific cases even-parity states have even been observed using synchrotron radiation sources [30,31]. Other processes such as double ionization can be ruled out as the second ionization energy (79.0 eV) [13] of He is more than double the photon energy. Sequential double excitation lacks a resonance level at the incident photon energy as He single ionization requires 24.6 eV and the lowest He double excitation 57.8 eV [32]. Likewise, excitation of the ground state He^+ ion by a second photon is prohibited by the lowest He^+ excitation energy ($1s \rightarrow 2p$) of 40.8 eV [13]. Also contributions of photoionization by higher FEL harmonics can be ruled out as the higher FEL harmonics are efficiently suppressed with the Al filter.

The additional feature in the photoelectron spectrum is not observed in the single-micropulse mode. After the two-photon excitation, the nonradiative (autoionization) and radiative decay channels lead both to ionized and neutrally excited helium, which are mainly singly excited levels ($N=1$) and a smaller fraction of doubly excited levels ($N=2$), respectively. However, at 2×10^{-5} mbar He pressure Coulomb repulsion among the ions clears the interaction volume as these ions travel between 10–20 mm within the $1 \mu\text{s}$ microbunch spacing. In contrast, the neutral helium expands thermally, traveling only 2 mm. Hence the next microbunch will interact not only with newly introduced helium from the gas doser but also with the neutral excited helium ($N=1$ and 2) originating from the initial doubly excited levels ($N=5$ and 6). Interaction of the excited helium ($N=1$ and 2) with the radiation results in resonant photoexcitation from the excited ($N=1$) levels into ($N=2$) levels and photoionization from the excited levels ($N=1$ and 2). If in the direct radiative decay from the initial excited levels ($N=5$ and 6) [Fig. 2(c), broken arrow] or in a chain photon processes involving the resonant photoexcitation and radiative decay channels between the excited ($N=1$) and ($N=2$) levels [33], neutral excited helium ($N=2$) in the vicinity of the He^+ ($N=2$) ionization threshold at 65.4 eV is produced, photoelectrons with kinetic energy between 24 and 26 eV can be emitted by single-photoionization [Fig. 2(c), right (blue) arrow]. The inner electron has a larger ionization cross section in this photon energy than the outer one in an independent electron model [34].

In conclusion we have investigated photoemission of helium with intense extreme ultraviolet radiation from FLASH. The spectral feature observed between 24 and 26 eV electron kinetic energy is explained as a result of subsequent processes involving a resonant two-photon absorption process into the doubly excited levels of even-parity ($N=5$ and 6) and finally the single photoionization of the doubly excited states in the vicinity of the He^+ ($N=2$) ionization threshold by the radiation of the next microbunches. This observation suggests that even-parity states, which have been elusive to be measured with the low pulse energy of synchrotron radiation sources, can be investigated with the intense radiation of FLASH. This also demonstrates a first step to bring nonlinear spectroscopy into the xuv and soft-x-ray regime.

Special thanks are due to the scientific and technical staff of the FLASH facility, especially to K. Rehlich, and V. Kocharyan, and V. Rybnikov. This work was supported by the German Ministry of Education and Research through Grants No. 05 KS4GU1/8 and No. 05 KS4GU1/9 and the Helmholtz joint Research Center “Physics with coherent radiation sources.”

- [1] H. C. Kapteyn, M. M. Murnane, and I. P. Christov, *Phys. Today* **58**(3), 39 (2005).
- [2] T. Brabec and F. Krausz, *Rev. Mod. Phys.* **72**, 545 (2000).
- [3] N. Bloembergen, *Rev. Mod. Phys.* **54**, 685 (1982).
- [4] A. H. Zewail, *J. Phys. Chem. A* **104**, 5660 (2000).
- [5] T. Laarmann, A. R. B. de Castro, P. Gurtler, W. Laasch, J. Schulz, H. Wabnitz, and T. Moller, *Phys. Rev. A* **72**, 023409 (2005).
- [6] A. R. B. de Castro, T. Laarmann, J. Schulz, H. Wabnitz, and T. Moller, *Phys. Rev. A* **72**, 023410 (2005).
- [7] T. Sekikawa, A. Kosuge, T. Kanai, and S. Watanabe, *Nature (London)* **432**, 605 (2004).
- [8] Y. Nabekawa, H. Hasegawa, E. J. Takahashi, and K. Midorikawa, *Phys. Rev. Lett.* **94**, 043001 (2005).
- [9] R. P. Madden and K. Codling, *Phys. Rev. Lett.* **10**, 516 (1963).
- [10] B. Zhou and C. D. Lin, *Phys. Rev. A* **49**, 1057 (1994).
- [11] T. K. Fang and T. N. Chang, *Phys. Rev. A* **56**, 1650 (1997).
- [12] J.-Z. Tang and I. Shimamura, *Phys. Rev. A* **50**, 1321 (1994).
- [13] M. Domke, K. Schulz, G. Remmers, G. Kaindl, and D. Wintgen, *Phys. Rev. A* **53**, 1424 (1996).
- [14] J.-E. Rubensson, C. S athe, S. Cramm, B. Kessler, S. Stranges, R. Richter, M. Alagia, and M. Coreno, *Phys. Rev. Lett.* **83**, 947 (1999).
- [15] T. W. Gorczyca, J.-E. Rubensson, C. S athe, M. Strom, M. Agaker, D. Ding, S. Stranges, R. Richter, and M. Alagia, *Phys. Rev. Lett.* **85**, 1202 (2000).
- [16] J. R. Harries, J. P. Sullivan, and Y. Azuma, *J. Phys. B* **37**, L169 (2004).
- [17] M. K. Odling-Smee, E. Sokell, P. Hammond, and M. A. MacDonald, *Phys. Rev. Lett.* **84**, 2598 (2000).
- [18] M. Coreno, K. C. Prince, R. Richter, M. de Simone, K. Bucar, and M. Zitnik, *Phys. Rev. A* **72**, 052512 (2005).
- [19] S. A. Collins *et al.*, *Phys. Rev. A* **65**, 052717 (2002).
- [20] F. Penent, P. Lablanquie, R. I. Hall, M.  itnik, K. Bu ar, S. Stranges, R. Richter, M. Alagia, P. Hammond, and J. G. Lambourne, *Phys. Rev. Lett.* **86**, 2758 (2001).
- [21] J. G. Lambourne *et al.*, *Phys. Rev. Lett.* **90**, 153004 (2003).
- [22] R. P uttner, B. Gr emaud, D. Delande, M. Domke, M. Martins, A. S. Schlachter, and G. Kaindl, *Phys. Rev. Lett.* **86**, 3747 (2001).
- [23] L. A. A. Nikolopoulos and P. Lambropoulos, *J. Phys. B* **34**, 545 (2001).
- [24] V. Ayvazyan *et al.*, *Eur. Phys. J. D* **37**, 297 (2006).
- [25] M. Martins, M. Wellhofer, J. T. Hoeft, W. Wurth, J. Feldhaus, and R. Follath, *Rev. Sci. Instrum.* **77**, 115108 (2006).
- [26] S. D usterer *et al.*, *Opt. Lett.* **31**, 1750 (2006).
- [27] The relative intensity $I_{2nd/1st}$ of the second harmonic to the fundamental behind the Al filter is given by $I_{2nd/1st} = I(0)_{2nd/1st} Tr_{2nd/1st}$, where $I(0)_{2nd/1st}$ is the relative intensity of the second harmonic to the fundamental in the FEL radiation and $Tr_{2nd/1st}$ is the relative transmission of the second harmonic to the fundamental through the Al filter. $I(0)_{2nd/1st}$ is 1.3×10^{-3} , which is obtained from M. Wellh ofer, M. Martins, W. Wurth, A. A-Sorokin, and M. Richter (unpublished). The transmission of the 700-nm-thick Al filter is 0.2 for the fundamental and 7×10^{-7} for the second harmonic, which are obtained from the Center for X-Ray Optics at Lawrence Berkeley Laboratory [B. L. Henke, E. M. Gullikson, and J. C. Davis, *At. Data Nucl. Data Tables* **54**, 181 (1993)]. Hence $Tr_{2nd/1st}$ is 3.5×10^{-6} and $I_{2nd/1st}$ is 5×10^{-9} .
- [28] M. Richter *et al.*, *Appl. Phys. Lett.* **83**, 2970 (2003).
- [29] J. A. R. Samson, Z. X. He, L. Yin, and G. N. Haddad, *J. Phys. B* **27**, 887 (1994).
- [30] B. Kr assig, E. P. Kanter, S. H. Southworth, R. Guillemin, O. Hemmers, D. W. Lindle, R. Wehlitz, and N. L. S. Martin, *Phys. Rev. Lett.* **88**, 203002 (2002).
- [31] K. C. Prince, M. Coreno, R. Richter, M. de Simone, V. Feyer, A. Kivimaki, A. Mihelic, and M. Zitnik, *Phys. Rev. Lett.* **96**, 093001 (2006).
- [32] M.-K. Chen, *Phys. Rev. A* **56**, 4537 (1997).
- [33] M. Nagasono (unpublished).
- [34] B. Zhou, C. D. Lin, J.-Z. Tang, S. Watanabe, and M. Matsuzawa, *J. Phys. B* **26**, L337 (1993).